AGU PUBLICATIONS

JGR

Journal of Geophysical Research: Space Physics

RESEARCH ARTICLE
10.1002/2015JA021718

Investigation of the Chirikov resonance overlap criteria for equatorial magnetosonic waves

S. N. Walker[1], M. A. Balikhin[1], P. Canu[2], N. Cornilleau-Wehrlin[2], and I. Moiseenko[3]

[1]Department of Automatic Control and Systems Engineering, University of Sheffield, Sheffield, UK, [2]Laboratoire de Physique des Plasmas, Ecole Polytechnique, Palaiseau, France, [3]Space Research Institute, Russian Academy of Sciences, Moscow, Russia

Key Points:
- EMWs have a discrete spectrum at harmonics of the proton gyrofrequency
- Diffusion tensors are modeled using quasi-linear theory which assumes a continuous wave spectrum
- The Chirikov resonance criteria are used to validate applicability of quasi-linear theory

Correspondence to:
S. N. Walker,
simon.walker@sheffield.ac.uk

Citation:
Walker, S. N., M. A. Balikhin, P. Canu, N. Cornilleau-Wehrlin, and I. Moiseenko (2015), Investigation of the Chirikov resonance overlap criteria for equatorial magnetosonic waves, *J. Geophys. Res. Space Physics*, *120*, 8774–8781, doi:10.1002/2015JA021718.

Received 22 JUL 2015
Accepted 8 OCT 2015
Accepted article online 11 OCT 2015
Published online 28 OCT 2015

Abstract Observations of equatorial magnetosonic waves made during the Cluster Inner Magnetospheric Campaign clearly show discrete spectra consisting of emissions around harmonics of the proton gyrofrequency. Equatorial magnetosonic waves are important because of their ability to efficiently scatter electrons in energy and pitch angle. This wave-particle interaction is numerically modeled through the use of diffusion coefficients, calculated based on a continuous spectrum such as that observed by spectrum analyzers. Using the Chirikov overlap resonance criterion, the calculation of the diffusion coefficient will be assessed to determine whether they should be calculated based on the discrete spectral features as opposed to a continuous spectrum. For the period studied, it is determined that the discrete nature of the waves does fulfill the Chirikov overlap criterion and so the use of quasi-linear theory with the assumption of a continuous frequency spectrum is valid for the calculation of diffusion coefficients.

1. Introduction

The understanding of the evolution of relativistic fluxes within the outer radiation belt is important for mitigation of deep surface charging effects on spacecraft hardware. Two complementary approaches are currently used to forecast the evolution of these electron fluxes. The first approach is empirical and involves the application of system science methodology to measurements of electron fluxes at GEO (Geostationary Earth Orbit) [e.g., *Balikhin et al.*, 2011; *Boynton et al.*, 2013]. While this method can provide an accurate forecast, it is only applicable at GEO where continuous measurements are available. The forecast outside GEO requires models that have been developed based on physical principles.

A number of numerical codes, such as VERB (Versatile Electron Radiation Belt) [*Shprits et al.*, 2008, 2009] or PADIE (Pitch Angle and Energy Diffusion of Ions and Electrons) [*Glauert and Horne*, 2005], have been developed to model the dynamics of relativistic electrons within the radiation belts. These codes are based on the solution of a set of diffusion equations and require tensors of the quasi-linear diffusion coefficients to account for particle interaction with various wave modes. The main types of waves that should be taken into account are chorus, hiss, equatorial magnetosonic waves (EMWs), and electromagnetic ion cyclotron waves.

This paper presents an observational study of EMW. A number of previous studies have concluded that EMW can contribute both to the acceleration and loss via the pitch angle scattering of high-energy electrons. Since their discovery [*Russell et al.*, 1970; *Gurnett*, 1976], it is known that EMWs exhibit a discrete spectrum consisting of a number of harmonics of the proton gyrofrequency (Ω_i). However, current computations of the diffusion coefficients required by numerical codes are estimated based on the assumption of a continuous EMW spectrum [see, e.g., *Shprits et al.*, 2013; *Mourenas et al.*, 2013]. The main goal is to check the validity of such assumption for the EMW emission using multispacecraft Cluster data obtained during the Inner Magnetosphere Campaign.

Equatorial magnetosonic waves were first observed by *Russell et al.* [1970] as oscillations in the magnetic field and later in electric field measurements [*Gurnett*, 1976] and were identified as highly obliquely propagating whistler mode waves that occurred at harmonics of the proton gyrofrequency between the proton gyrofrequency and lower hybrid frequency [*Perraut et al.*, 1982; *Laakso et al.*, 1990; *Horne et al.*, 2000; *Němec et al.*, 2005; *Balikhin et al.*, 2015]. Their highly oblique propagation causes these waves to be confined to within a few (<5) degrees of the magnetic equator. These emissions have been observed in conjunction with ring-like

proton distributions [*Perraut et al.*, 1982; *Santolík et al.*, 2002; *Meredith et al.*, 2008; *Chen et al.*, 2011; *Thomsen et al.*, 2011] that provide the free energy for their growth via resonance interactions, generating a spectrum of discrete emissions at harmonics of the proton gyrofrequency [*Balikhin et al.*, 2015].

The variability of the radiation belts is modeled numerically using transport codes to describe these wave-plasma interactions. In these codes, the effects of the waves on the particle population are characterized by tensors of diffusion coefficients, calculated using statistically modeled wave amplitudes and based on a quasi-linear treatment of the problem. The wave amplitudes that appear in these quasi-linear models are computed under the assumption that the observed wave spectrum possess a continuous spectrum in frequency space; i.e., the emissions are continuous. This is typically the case when considering data from a spectrum analyzer [see, e.g., *Mourenas et al.*, 2013, Figure 1] since these devices do not have sufficient narrowband spectral channels to resolve the true nature of these emissions. It is, however, possible to resolve these discrete emissions from waveform data provided that the sampling rate is sufficient to investigate the frequency range of the waves.

Equatorial magnetosonic waves resonantly interact with trapped electrons, providing an important mechanism for their acceleration and loss [*Thorne*, 2010]. While cyclotron resonance processes are unlikely be important due to the high energies (MeV) of the particles required, the interaction of the Landau resonance with a highly oblique electromagnetic wave may operate over a broader range of lower energies ($\sim$ 100 keV), efficiently violating the first adiabatic invariant. This process was demonstrated to be capable of accelerating particles on similar time scales as other wave modes [*Horne et al.*, 2007]. These resonant interactions have been investigated analytically using the quasi-linear approximation to determine expressions for the diffusion tensor coefficients used within numerical models. Quasi-linear diffusion theory predicts that pure pitch angle diffusion due to cyclotron resonances occurs when the parallel velocity of resonant electrons exceeds the wave parallel phase velocity [*Lyons et al.*, 1971] and is limited to cases of moderate-amplitude, broadband waves or ensemble averages (over many bounce periods) of narrowband emissions assuming that particle displacements may be considered stochastic [*Mourenas et al.*, 2013]. Test particle simulations of the Landau resonant interaction have shown similar results to the predictions of quasi-linear diffusion theory [*Bortnik and Thorne*, 2010; *Li et al.*, 2014].

The general expressions for quasi-linear pitch angle diffusion, originally derived by *Lyons* [1974] and reformulated by *Albert* [2005, 2007], are dependent upon the dispersion of EMW. In deriving the dispersion relation of whistler mode waves based on quasi-linear theory [*Lyons et al.*, 1971; *Lyons*, 1974] and incorporating simplifying assumptions based on observations [e.g., *Russell et al.*, 1970; *Boardsen et al.*, 1992; *Němec et al.*, 2005; *Horne et al.*, 2007; *Chen et al.*, 2011; *Mourenas et al.*, 2013], it was usually assumed that the wave spectrum was continuous. However, all previous authors did note that the observed spectrum would consist of discrete emissions at harmonics of the proton gyrofrequency. The use of the continuous spectrum, employed in quasi-linear theory, may, however, be justified providing that the harmonic elements satisfy the Chirikov resonance overlap criteria.

The Chirikov resonance overlap criteria [*Chirikov*, 1960] defines the chaos border in a Hamiltonian system. It states that a deterministic trajectory will begin to move between two nonlinear resonances in a Hamiltonian system in a chaotic and unpredictable manner as soon as these unperturbed resonances overlap. Physically, this implies that if the resonance widths of two adjacent harmonic emission bands are large enough in comparison with the fundamental frequency such that they overlap, i.e.,

$$S^2 > 1; S = \Delta\omega_r/\Omega_d \tag{1}$$

where $\Delta\omega_r$ is the frequency half width of the unperturbed resonance and Ω_d is the frequency distance between two unperturbed resonances, particles may move between different resonance frequencies in a chaotic manner and so may not be associated with one particular resonance which is the case when the emissions are discrete and well separated.

When considering the interaction of EMW with electrons in Landau resonance, overlap of neighboring harmonic emissions may occur for two adjacent resonances when [*Artemyev et al.*, 2015]

$$\delta\theta > \frac{v/\tan\theta_m}{1-\omega^2/v\Omega_{ce}^2} \tag{2}$$

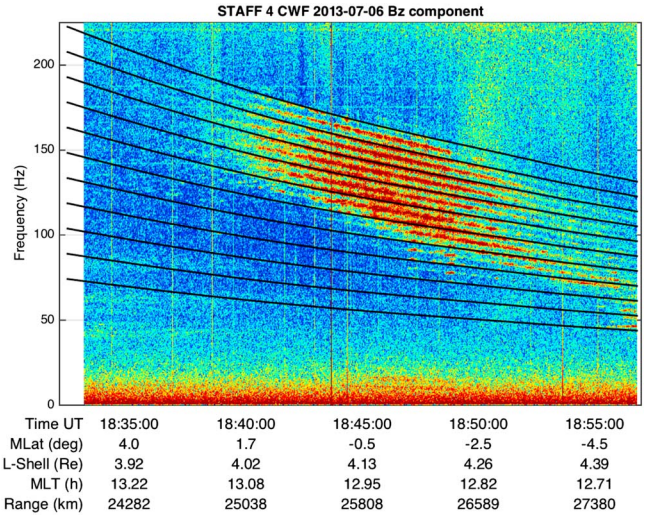

Figure 1. Dynamic spectrogram of the Cluster 4 STAFF search coil waveform measured on 6 July 2013 for the period 18:32–18:57 UT.

where θ_m is the mean angle between the propagation direction and the external magnetic field, $\delta\theta$ is the standard deviation of the wave propagation angles θ_m, l is the harmonic number, $\nu = m_e/m_p$ is the electron to proton mass ratio, and Ω_{ce} is the electron gyrofrequency. The values of θ_m and $\delta\theta$ are related to the width of the resonance (assuming small values of $\delta\theta$) by

$$\delta(\omega/k_{\|}) = \frac{\omega}{k_{\|}}\delta\theta \tan\theta_m \qquad (3)$$

If equation (2) is satisfied, it follows that the more general Chirikov resonance overlap criteria should be fulfilled and hence the use of quasi-linear theory justified in the analysis of these emissions. If, however, this criterion is not satisfied, then the contribution of each harmonic to the diffusion coefficient should be evaluated separately.

2. Observations

The data presented in this paper were collected as part of the Cluster Inner Magnetosphere Campaign which ran from July to October 2013. This study targeted observations of electric and magnetic field waves in order to investigate their nonlinear properties and interactions with the particle populations within the inner magnetosphere and to investigate the role of plasma waves in the processes of electron energization as well as loss from the radiation belts. During this campaign, the Cluster satellites were flying in a "100 km formation" in which two satellites (Cluster 3 and 4) are typically separated by around 30 km, an ideal situation for probing the wave environment.

The observations presented and analyzed here were made on 6 July 2013 between 18:32 and 18:57 UT and are shown in Figure 1. During this period, Cluster operated in burst science mode which provides fluxgate magnetometer [*Balogh et al.*, 1997] measurements of the background magnetic field with a sampling rate of 67 Hz, together with Spatio-Temporal Analysis of Field Fluctuations (STAFF) [*Cornilleau-Wehrlin et al.*, 1997] measurements of magnetic field oscillations sampled at 450 Hz. At this time the Cluster spacecraft were located at a radial distance of the order of 3.8–4.2 R_E on the dayside at a local time 1330–1250, crossing the magnetic equator at around 1844 UT in the direction north to south. During this observational period the magnitude of the external magnetic field changes gradually from 487 to 287 nT. Thus, the proton gyrofrequency changes from 7.4 to 4.4 Hz and the lower hybrid frequency from 318 to 187 Hz.

Figure 1 shows the dynamic spectrogram of measurements made by get STAFF search coil magnetometer. The black lines indicate harmonics of the local proton gyrofrequency in the range 10 to 30 in steps of 2. At around 18:40 UT a set of banded emissions begin to be observed at frequencies in the range 130–180 Hz. The exact frequencies of the wave correspond approximately to the 21st to 30th harmonics of the local proton gyrofrequency. At this time, Cluster 4 is situated at a magnetic latitude of 1.7°N and approximately 13:13 magnetic local time, traveling in a southward direction. As the satellite approaches the magnetic equator the emission bands intensify reaching a maximum as Cluster 4 is located about 1°S of the magnetic equator, before beginning to disappear from around 18:52 UT onward. During these observations the proton gyrofrequency decreases notably. This change is also observed in the emission frequency of the waves. On closer inspection, the exact frequency of emission appears just below the harmonic frequency when the waves are first observed. As Cluster 4 crosses the magnetic equator, the emission frequency rises to the exact harmonic frequency before dropping below it again as the satellite continues on its southward trajectory. The fact that the emissions follow the proton harmonic frequencies so closely is taken as evidence that these emissions were observed in the source region of the waves. Toward the end of the observational period at 18:56 UT

banded emissions are observed at the 10th to 14th harmonics of the local gyrofrequency. In contrast to the earlier emissions, these bands show a constant frequency of emission, indicative that they have propagated from their source region to the location at which they were observed.

3. Analysis Methodology

In this paper, the Chirikov resonance overlap parameter is investigated in relation to the harmonic nature of these discrete emissions using the overlap parameter formulated in *Artemyev et al.* [2015]. As mentioned in section 1, magnetosonic waves play an important role in the energization and loss processes within the radiation belts. In order to incorporate these features into numerical models, a set of quasi-linear diffusion coefficients are computed based on the results of statistical surveys of the occurrence and amplitude of these waves [*Meredith et al.*, 2008; *Mourenas et al.*, 2013]. These surveys assume that the spectrum of the magnetosonic waves can be considered as continuous in frequency space, and hence, the resulting set of diffusion coefficients may be estimated based on quasi-linear theory. However, the discrete nature of the magnetosonic emissions means that this approach may generate erroneous results unless the Chirikov resonance overlap parameter for stochastic motion is satisfied.

The validity of equation (2) was tested on two short (10 s) periods of observations to ensure that the frequency of emission did not change significantly. The components of the STAFF magnetic waveform signal were first transformed into the frequency domain using the Morlet wavelet transform. Evaluation of the overlap criteria is based on the mean and distribution of the wave normal angles at each of the discrete emission frequencies corresponding to peaks in the wavelet spectra. The wave normal angles were determined using two methods. The first involves dividing the wavelet filtered waveform for the whole period into intervals of 0.25 s (typically containing 112 data points). For each interval whose mean amplitude was above a certain threshold (see later) a minimum variance analysis (MVA) was performed to determine the direction of minimum variance which, for magnetic field measurements, corresponds to the propagation direction of the wave. In order to ensure that the minimum variance direction is well determined, only those vectors for which the ratio of the intermediate to minimum eigenvalues exceeded 10 were used. The methodology used to estimate the angular error $|\Delta\phi_{ij}|$ between eigenvectors *i* and *j* resulting from the MVA technique is that developed by *Sonnerup and Scheible* [1998]. For the minimum variance direction, the expected angular uncertainties with respect to the maximum and intermediate variance axes are within the ranges $0.0007 < |\Delta\phi_{13}| < 0.37°$ (average $\approx 0.038°$) and $0.021 < |\Delta\phi_{23}| < 1.83°$ (average $\approx 0.60°$), respectively. In all individual time intervals considered, the uncertainty $|\Delta\phi_{13}|$ was smaller than $|\Delta\phi_{23}|$. In order to analyze the effects of large values of $|\Delta\phi_{23}|$, a further constraint was added for MVA, namely, $|\Delta\phi_{23}| < 0.6°$. The resulting sets of propagation angles obtained from MVA with respect to the external magnetic field (θ_{Bk}) were then analyzed to determine the mean direction of propagation (θ_m) and its standard deviation as a measure of its variance ($\delta\theta$).

The second method used to determine the wave normal angles was calculated using singular value decomposition (SVD) of the full spectral matrix [*Santolik et al.*, 2003].

Table 1 shows an example of how the values of the mean (θ_m), standard deviation of the distribution ($\delta\theta$), and right-hand side of equation (2) vary as the threshold of the wave amplitude/trace is increased for signals at a frequency of 103 Hz during the period 18:47:05–18:47:15 UT. The first column defines the threshold level in terms of the maximum amplitude (MVA) of the waveform or trace of the spectral matrix (SVD) for the period analyzed. The second column gives the number of intervals (MVA) or points (SVD) used for the determination of the mean and standard deviation of the wave normal direction, which are shown in the third and fourth columns. Finally, the fifth column shows the value of the right-hand side (RHS) of equation (2). These results show that while the average direction (θ_m) remains fairly constant as the threshold is increased, the standard deviation ($\delta\theta$) changes considerably. Below a threshold of 0.2 the dispersion of the distribution is large, probably due to the influence of low-amplitude noise on the results. As the threshold is increased above 0.2, the values of θ_m and $\delta\theta$ do not vary greatly; however, the number of values used in their determination falls significantly. Thus, the results of the analysis discussed in this paper are based on data in which the amplitude/trace is greater than a threshold value of 0.2. In the case of MVA, there were typically 20–35 (out of 40) data points contributing to the statistics, while for the SVD analysis the number of points was 5000–7000 (out of 9000) in each interval.

Table 1. Variation of θ_m, $\delta\theta$, and the Ratio $\frac{\nu l/\tan\theta_m}{1-\omega^2/\nu\Omega_{ce}^2}$ as the Minimum Wave Amplitude Is Increased[a]

	Minimum Amplitude	# Points	θ_m (deg)	$\delta\theta$ (deg)	Ratio
MVA	0.1	36	88.00	1.48	0.026
	0.2	24	88.29	0.94	0.022
	0.3	17	88.22	1.01	0.023
	0.4	14	88.17	1.10	0.024
	0.5	12	88.04	1.13	0.025
	0.6	10	87.82	1.04	0.028
	0.7	8	88.04	1.03	0.026
SVD	0.1	8447	87.28	3.12	0.035
	0.2	5992	88.30	0.87	0.022
	0.3	4392	88.30	0.80	0.022
	0.4	3847	88.31	0.82	0.022
	0.5	3525	88.27	0.82	0.022
	0.6	2877	88.12	0.76	0.024
	0.7	2424	88.22	0.75	0.023

[a]The results correspond to a frequency of 103 Hz for the time period 18:47:05–18:47:15 UT.

4. Results

The EMW emissions presented here were mainly observed in the B_x and B_z GSE components. Figure 2 shows the Fourier spectrum of the B_x (GSE) component of the magnetic field measured by the STAFF search coil magnetometer on satellite 4 during the period 18:45:00–18:45:10 UT on 6 July 2013. This spectrum represents the mean power based on four 1024-point fast Fourier transforms (FFTs). The vertical dotted lines indicate the 18th–30th harmonics of the proton gyrofrequency averaged during this observation period (5.53 Hz) as labeled toward the bottom of this figure. This spectrum clearly shows the discrete, banded nature of the magnetosonic waves, as opposed to one possessing a continuous distribution in frequency space. These strong emissions, observed at frequencies close to the 18th–29th harmonics of the proton gyrofrequency, are around 3 orders of magnitude more powerful than the background level of the spectrum. The lower harmonics (19–24) tend to show the peak intensities slightly above the proton gyrofrequency harmonics, while those above occur at or slightly below the harmonic frequencies. However, investigation of these subtle frequency shifts with respect to the harming frequencies is beyond the scope of the current paper.

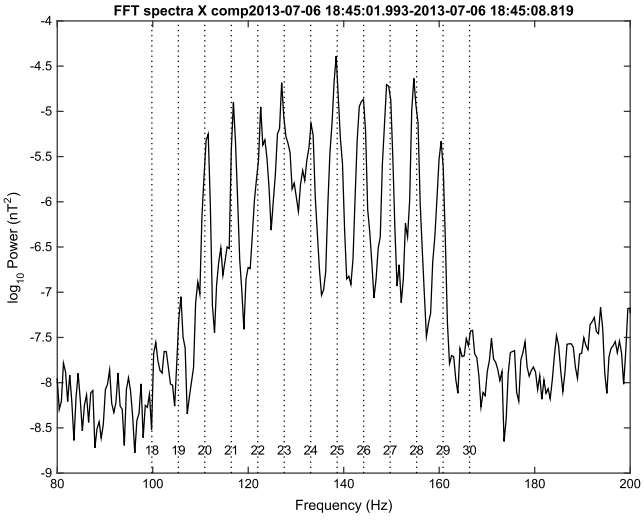

Figure 2. FFT spectrum of Cluster 4 waveform observations of magnetosonic waves on 6 July 2013 for the period 18:45:00–18:45:10 UT.

Figure 3 shows the results of calculating the overlap criteria defined by equation (2) as a function of the harmonic number l for observations in the period 18:45:00–18:45:10. The red and blue crosses represent the RHS of equation (2) based on values of the distribution of the angle between the wave propagation vector and the external magnetic field resulting from MVA and SVD, respectively. The red and blue

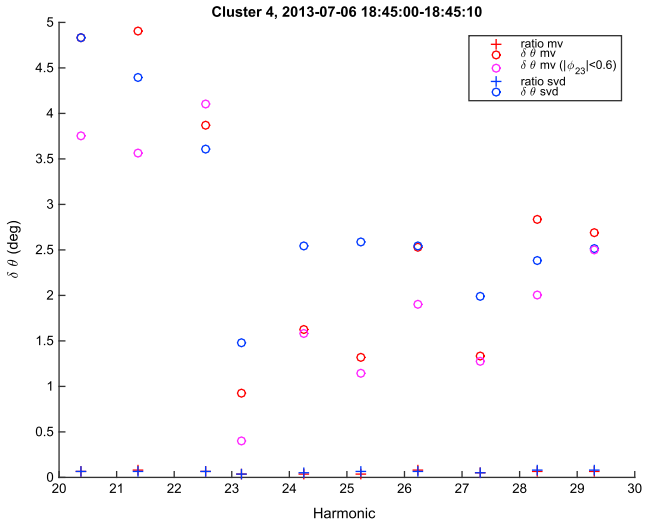

Figure 3. Results of the analysis of the overlap criteria for observations in the period 18:45:00–18:45:10. The red and blue crosses represent the RHS of equation (2) based on values of the distribution of the angle between the wave propagation vector and the external magnetic field resulting from MVA and SVD, respectively. The red and blue circles represent the standard deviation of the angular distribution resulting from MVA and SVD, respectively. The magenta circles show the standard deviation of the wave vector directions when the extra constraint $|\phi_{23}| < 0.6$ is applied to the variance analysis.

circles represent the standard deviation of the angular distribution resulting from MVA and SVD, respectively. The magenta circles show the values of $\delta\theta$ resulting from MVA when the extra constraint $|\phi_{23}| < 0.6$ was included. Generally, this tends to remove some of the outlying wave propagation angles, resulting in a narrower distribution and hence reduced values of $\delta\theta$ as is shown in Figure 3. Since the values of $\delta\theta$ are still much greater than the largest errors that may result from MVA, we can conclude that the apparent spread of wave vector directions with respect to the external magnetic field is not due to the propagation of errors resulting from MVA. Even with the addition of this extra constraint, the values of $\delta\theta$ are still around an order of magnitude greater than the value resulting from the RHS of equation (2), and thus, our conclusions are unaffected. From Figure 3, it is clear that the criterion in equation (2) is always fulfilled, implying that the stochastic scattering of particles by EMW with a discrete frequency spectrum occurs. Since equation (2) is satisfied, the Chirikov resonance overlap criteria will be satisfied. Hence, the waves may be considered to possess a continuous spectrum for the calculation of quasi-linear diffusion coefficients from wave measurements.

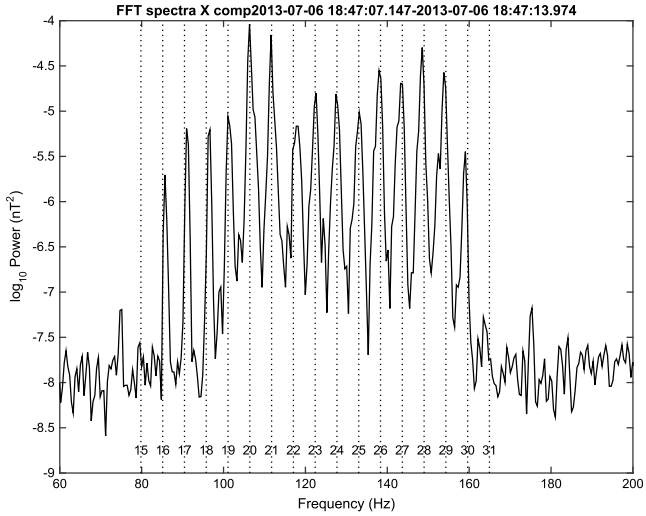

Figure 4. FFT spectrum of Cluster 4 waveform observations of magnetosonic waves on 6 July 2013 for the period 18:47:05–18:47:15 UT.

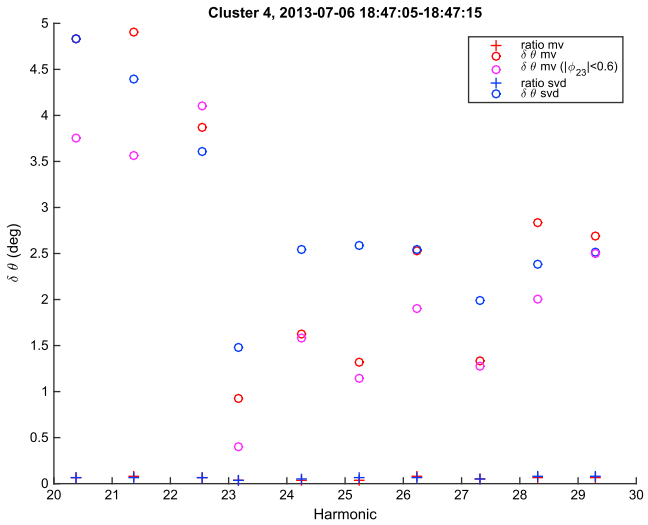

Figure 5. Same as Figure 3 based on data from the period 18:47:05–18:47:15.

Figure 4 shows a second-average wave spectrum observed between 18:47:05 and 18:47:15 on the same day. During this period the mean proton gyrofrequency was 5.13 Hz. Emissions were observed between the 16th and 33rd harmonics of the proton gyrofrequency. The results of the analysis of the resonance condition equation (2) are shown in Figure 5, using the same format as Figure 3. Again, it shows that the overlap condition is satisfied for this set of observations.

5. Discussion and Conclusions

During the Cluster Inner Magnetospheric Campaign three of the four satellites observed emissions at multiple harmonics of the proton gyrofrequency. These discrete emissions correspond to equatorial magnetosonic waves that propagate almost perpendicularly to the external magnetic field; their oscillating magnetic field is aligned with the external field and is confined to the equatorial region.

It has been shown [e.g., *Horne et al.*, 2007] that EMW can interact with electrons within the radiation belts. Interacting through the Landau resonance, this wave mode may be responsible for the acceleration of a subset of particles to high energies while scattering other particles into the loss cone enabling their subsequent loss from the radiation belts. Within numerical models of the radiation belts, these wave-particle interactions are characterized by sets of diffusion tensors, calculated from a quasi-linear description of the plasma. The approach usually employed by, e.g., *Horne et al.* [2007] assumes that the observed waves can be described using a continuous frequency spectrum rather than as a set of discrete emissions. Since EMW possess a discrete emission spectra, it is not obvious whether the assumption of a continuous spectrum is valid or not. By analyzing the spectrum of emissions in terms of the Chirikov resonance overlap condition, this paper has investigated the validity of the continuous spectrum assumption.

It is evident from Figures 2 and 4 that EMWs are composed of discrete emissions at high (18th–30th) harmonics of the proton gyrofrequency. These emissions may be treated using the quasi-linear approximation assuming that the Chirikov resonance overlap criteria (equation (1)) are fulfilled. Analysis of the observed wave emissions observed by Cluster 4 on 6 July 2013 presented here shows that in this instance, the resonance overlap criteria are fulfilled. Since the value of $\delta\theta$ resulting equation (2) is observed to be small (typically $\delta\theta < 0.05°$), it appears that the stochastic scattering of charged particles by EMW may take place for almost all but the narrowest of discrete emission bands.

Acknowledgments
S.N.W. and M.A.B. wish to acknowledge financial support from International Space Science Institute, Bern, Royal Society Collaboration grant and the UK EPSRC under grant EP/H00453X/1. M.A.B. and S.N.W. also wish to acknowledge A.V. Artemyev for useful discussions regarding the analysis presented here. The authors would like to thank the Cluster instrument teams for provision of the data used in this paper. These data are available from the Cluster Science Archive (http://www.cosmos.esa.int/web/csa).

References

Albert, J. M. (2005), Evaluation of quasi-linear diffusion coefficients for whistler mode waves in a plasma with arbitrary density ratio, *J. Geophys. Res.*, *110*, A03218, doi:10.1029/2004JA010844.

Albert, J. M. (2007), Simple approximations of quasi-linear diffusion coefficients, *J. Geophys. Res.*, *112*, A12202, doi:10.1029/2007JA012551.

Artemyev, A. V., D. Mourenas, O. V. Agapitov, and V. V. Krasnoselskikh (2015), Relativistic electron scattering by magnetosonic waves: Effects of discrete wave emission and high wave amplitudes, *Phys. Plasmas*, *22*, 62901, doi:10.1063/1.4922061.

Balikhin, M. A., R. J. Boynton, S. N. Walker, J. E. Borovsky, S. A. Billings, and H. L. Wei (2011), Using the NARMAX approach to model the evolution of energetic electrons fluxes at geostationary orbit, *Geophys. Res. Lett.*, *38*, L18105, doi:10.1029/2011GL048980.

Balikhin, M. A., Y. Y. Shprits, S. N. Walker, L. Chen, N. Cornilleau-Wehrlin, I. Dandouras, O. Santolik, C. Carr, K. H. Yearby, and B. Weiss (2015), Observations of discrete harmonics emerging from equatorial noise, *Nat. Commun.*, *6*, 7703, doi:10.1038/ncomms8703.

Balogh, A., et al. (1997), The Cluster magnetic field investigation, *Space Sci. Rev.*, *79*, 65–91, doi:10.1023/A:1004970907748.

Boardsen, S. A., D. L. Gallagher, D. A. Gurnett, W. K. Peterson, and J. L. Green (1992), Funnel-shaped, low-frequency equatorial waves, *J. Geophys. Res.*, *97*, 14,967–14,976, doi:10.1029/92JA00827.

Bortnik, J., and R. M. Thorne (2010), Transit time scattering of energetic electrons due to equatorially confined magnetosonic waves, *J. Geophys. Res.*, *115*, A07213, doi:10.1029/2010JA015283.

Boynton, R. J., M. A. Balikhin, S. A. Billings, G. D. Reeves, N. Ganushkina, M. Gedalin, O. A. Amariutei, J. E. Borovsky, and S. N. Walker (2013), The analysis of electron fluxes at geosynchronous orbit employing a NARMAX approach, *J. Geophys. Res. Space Physics*, *118*, 1500–1513, doi:10.1002/jgra.50192.

Chen, L., R. M. Thorne, V. K. Jordanova, M. F. Thomsen, and R. B. Horne (2011), Magnetosonic wave instability analysis for proton ring distributions observed by the LANL magnetospheric plasma analyzer, *J. Geophys. Res.*, *116*, A03223, doi:10.1029/2010JA016068.

Chirikov, B. V. (1960), Resonance processes in magnetic traps, *J. Nucl. Energy Part C*, *1*, 253–260.

Cornilleau-Wehrlin, N., et al. (1997), The Cluster Spatio-Temporal Analysis of Field Fluctuations (STAFF) experiment, *Space Sci. Rev.*, *79*, 107–136.

Glauert, S. A., and R. B. Horne (2005), Calculation of pitch angle and energy diffusion coefficients with the PADIE code, *J. Geophys. Res.*, *110*, A04206, doi:10.1029/2004JA010851.

Gurnett, D. A. (1976), Plasma wave interactions with energetic ions near the magnetic equator, *J. Geophys. Res.*, *81*, 2765–2770, doi:10.1029/JA081i016p02765.

Horne, R. B., G. V. Wheeler, and H. S. C. K. Alleyne (2000), Proton and electron heating by radially propagating fast magnetosonic waves, *J. Geophys. Res.*, *105*, 27,597–27,610, doi:10.1029/2000JA000018.

Horne, R. B., R. M. Thorne, S. A. Glauert, N. P. Meredith, D. Pokhotelov, and O. Santolík (2007), Electron acceleration in the Van Allen radiation belts by fast magnetosonic waves, *Geophys. Res. Lett.*, *34*, L17107, doi:10.1029/2007GL030267.

Laakso, H., H. Junginger, R. Schmidt, A. Roux, and C. de Villedary (1990), Magnetosonic waves above $f_c(H^+)$ at geostationary orbit: GEOS 2 results, *J. Geophys. Res.*, *95*, 10,609–10,621, doi:10.1029/JA095iA07p10609.

Li, J., et al. (2014), Interactions between magnetosonic waves and radiation belt electrons: Comparisons of quasi-linear calculations with test particle simulations, *Geophys. Res. Lett.*, *41*, 4828–4834, doi:10.1002/2014GL060461.

Lyons, L. R. (1974), Pitch angle and energy diffusion coefficients from resonant interactions with ion–cyclotron and whistler waves, *J. Plasma Phys.*, *12*, 417–432, doi:10.1017/S002237780002537X.

Lyons, L. R., R. M. Thorne, and C. F. Kennel (1971), Electron pitch-angle diffusion driven by oblique whistler-mode turbulence, *J. Plasma Phys.*, *6*, 589–606, doi:10.1017/S0022377800006310.

Meredith, N. P., R. B. Horne, and R. R. Anderson (2008), Survey of magnetosonic waves and proton ring distributions in the Earth's inner magnetosphere, *J. Geophys. Res.*, *113*, A06213, doi:10.1029/2007JA012975.

Mourenas, D., A. V. Artemyev, O. V. Agapitov, and V. Krasnoselskikh (2013), Analytical estimates of electron quasi-linear diffusion by fast magnetosonic waves, *J. Geophys. Res. Space Physics*, *118*, 3096–3112, doi:10.1002/jgra.50349.

Němec, F., O. Santolík, K. Gereová, E. Macúšová, Y. de Conchy, and N. Cornilleau-Wehrlin (2005), Initial results of a survey of equatorial noise emissions observed by the Cluster spacecraft, *Planet. Space Sci.*, *53*, 291–298, doi:10.1016/j.pss.2004.09.055.

Perraut, S., A. Roux, P. Robert, R. Gendrin, J. A. Sauvaud, J. M. Bosqued, G. Kremser, and A. Korth (1982), A systematic study of ULF waves above f_{H^+} from GEOS 1 and 2 measurements and their relationship with proton ring distributions, *J. Geophys. Res. A*, *87*, 6219–6236.

Russell, C. T., R. E. Holzer, and E. J. Smith (1970), OGO 3 observations of ELF noise in the magnetosphere: 2. The nature of the equatorial noise, *J. Geophys. Res.*, *75*, 755–768, doi:10.1029/JA075i004p00755.

Santolík, O., J. S. Pickett, D. A. Gurnett, M. Maksimovic, and N. Cornilleau-Wehrlin (2002), Spatiotemporal variability and propagation of equatorial noise observed by Cluster, *J. Geophys. Res.*, *107*(A12), 1495, doi:10.1029/2001JA009159.

Santolik, O., M. Parrot, and F. Lefeuvre (2003), Singular value decomposition methods for wave propagation analysis, *Radio Sci.*, *38*(1), 1010, doi:10.1029/2000RS002523.

Shprits, Y. Y., S. R. Elkington, N. P. Meredith, and D. A. Subbotin (2008), Review of modeling of losses and sources of relativistic electrons in the outer radiation belt: I. Radial transport, *J. Atmos. Sol. Terr. Phys.*, *70*, 1679–1693, doi:10.1016/j.jastp.2008.06.008.

Shprits, Y. Y., D. Subbotin, and B. Ni (2009), Evolution of electron fluxes in the outer radiation belt computed with the VERB code, *J. Geophys. Res.*, *114*, A11209, doi:10.1029/2008JA013784.

Shprits, Y. Y., A. Runov, and B. Ni (2013), Gyro-resonant scattering of radiation belt electrons during the solar minimum by fast magnetosonic waves, *J. Geophys. Res. Space Physics*, *118*, 648–652, doi:10.1002/jgra.50108.

Sonnerup, B. U. Ö., and M. Scheible (1998), Minimum and maximum variance analysis, in *Analysis Methods for Multispacecraft Data, ISSI Sci. Rep. Ser.*, vol. *SR-001*, edited by G. Paschmann and P. W. Daly, pp. 185–220, ISSI/ESA, Dartmouth College Hanover, N. H.

Thomsen, M. F., M. H. Denton, V. K. Jordanova, L. Chen, and R. M. Thorne (2011), Free energy to drive equatorial magnetosonic wave instability at geosynchronous orbit, *J. Geophys. Res.*, *116*, A08220, doi:10.1029/2011JA016644.

Thorne, R. M. (2010), Radiation belt dynamics: The importance of wave-particle interactions, *Geophys. Res. Lett.*, *37*, L22107, doi:10.1029/2010GL044990.